

cent secondary antibodies were diluted 1/200, with the exception of that shown in Fig. 3f–k, where Texas-red-labelled antibodies were diluted 1/700. Figures 2e–g and 3a, c–k represent individual confocal sections. The mouse monoclonal antibodies to tubulin and Myc were TUB2.1 (Sigma) and 9E10, respectively. Rabbit antibodies to RhoA (Santa Cruz) were diluted 1/100 times. Fluorescence intensity in individual cells was measured by a camera attached to the fluorescence microscope (Axiohot, Zeiss). A transfected cell was considered as highly expressing a protein if it required an exposure time of less than 10 s. This value was observed in ~20% of the transfected cells. The rate of spontaneous cytokinesis failure, 1.8%, was estimated with control cells cotransfected with 1 µg pCAG-MycSTOP and 100 ng pEGFP-C1 (Clontech).

Flow cytometry. Two days after transfection, cells were trypsinized, fixed with 0.5% formaldehyde and permeabilized with 0.1% Triton X-100. They were stained for recombinant citron with antibodies to Myc and FITC-conjugated secondary antibodies, and for DNA with propidium iodide. The stained cells were subjected to flow cytometry on a FACSCalibur (Becton Dickinson). Citron-transfected cells positive for FITC and mock-transfected cells were analysed for DNA content.

Effect of Y-27632 on cytokinesis. HeLa cells were synchronized with thymidine and nocodazole as described²⁸. After this procedure, ~60% of the cells appeared to have arrested in the M phase of the cell cycle. Y-27632 was added to the culture medium at various concentrations for the last 30 min of the nocodazole incubation. Cells were then washed three times and incubated with medium containing Y-27632 for 3 h. The percentage of mitotic cells that became binucleate was determined visually.

Received 5 May; accepted 17 June 1998.

- Mabuchi, I. Biochemical aspects of cytokinesis. *Int. Rev. Cytol.* **101**, 175–213 (1986).
- Satterwhite, L. L. & Pollard, T. D. Cytokinesis. *Curr. Opin. Cell Biol.* **4**, 43–52 (1992).
- Fishkind, D. J. & Wang, Y.-L. New horizons for cytokinesis. *Curr. Opin. Cell Biol.* **7**, 23–31 (1995).
- Byer, B. & Abramson, D. H. Cytokinesis in HeLa: post-telophase delay and microtubule-associated motility. *Protoplasma* **66**, 413–435 (1968).
- Mullins, J. M. & Bieseis, J. J. Terminal phase of cytokinesis in D-98S cells. *J. Cell Biol.* **73**, 672–684 (1977).
- Machesky, L. M. & Hall, A. Rho: a connection between membrane receptor signalling and the cytoskeleton. *Trends Cell Biol.* **6**, 304–310 (1996).
- Narumiya, S. The small GTPase Rho: cellular functions and signal transduction. *J. Biochem. (Tokyo)* **120**, 215–228 (1996).
- Mabuchi, I. *et al.* A rho-like protein is involved in the organisation of the contractile ring in dividing sand dollar eggs. *Zygote* **1**, 325–331 (1993).
- Kishi, K., Sasaki, T., Kuroda, S., Itoh, T. & Takai, Y. Regulation of cytoplasmic division of *Xenopus* embryo by rho p21 and its inhibitory GDP/GTP exchange protein (rho GDI). *J. Cell Biol.* **120**, 1187–1195 (1993).
- Drechsel, D. N., Hyman, A. A., Hall, A. & Glotzer, M. A requirement for Rho and Cdc42 during cytokinesis in *Xenopus* embryos. *Curr. Biol.* **7**, 12–23 (1996).
- Terada, Y. *et al.* AIM-1: a mammalian midbody associated protein required for cytokinesis. *EMBO J.* **17**, 667–676 (1998).
- Sekimata, M. *et al.* Detection of protein kinase activity specifically activated at metaphase-anaphase transition. *J. Cell Biol.* **132**, 635–641 (1996).
- Madaule, P. *et al.* A novel partner for the GTP-bound forms of rho and rac. *FEBS Lett.* **377**, 243–248 (1995).
- Ishizaki, T. *et al.* The small GTP-binding protein Rho binds to and activates a 160 kDa Ser/Thr protein kinase homologous to myotonic dystrophy kinase. *EMBO J.* **15**, 1885–1893 (1996).
- Leung, T., Manser, E., Tan, L. & Lim, L. A novel serine/threonine kinase binding the Ras-related RhoA GTPase which translocates the kinase to peripheral membranes. *J. Biol. Chem.* **270**, 29051–29054 (1995).
- Matsuji, T. *et al.* Rho-associated kinase, a novel serine/threonine kinase, as a putative target for the small GTP binding protein Rho. *EMBO J.* **15**, 2208–2216 (1996).
- Nakagawa, O. *et al.* ROCK-I and ROCK-II: two isoforms of Rho-associated coiled-coil forming protein serine/threonine kinase in mice. *FEBS Lett.* **392**, 189–193 (1996).
- Ishizaki, T. *et al.* p160ROCK, a Rho-associated coiled-coil forming protein kinase, works downstream of Rho and induces focal adhesions. *FEBS Lett.* **404**, 118–124 (1997).
- Leung, T., Chen, X.-Q., Manser, E. & Lim, L. The p160 RhoA-bindin kinase ROKα is a member of a kinase family and is involved in the reorganization of the cytoskeleton. *Mol. Cell. Biol.* **16**, 5313–5327 (1996).
- Kimura, K. *et al.* Regulation of myosin phosphatase by Rho and Rho-associated kinase (Rho-kinase). *Science* **273**, 245–248 (1996).
- Kureishi, Y. *et al.* Rho-associated kinase directly induces smooth muscle contraction through myosin light chain phosphorylation. *J. Biol. Chem.* **272**, 12257–12260 (1997).
- Luo, L. *et al.* Genghis Khan (Gek) as a putative effector for *Drosophila* Cdc42 and regulator of actin polymerisation. *Proc. Natl Acad. Sci. USA* **94**, 12963–12968 (1997).
- Leung, T., Chen, X.-Q., Tan, I., Manser, E. & Lim, L. Myotonic dystrophy kinase-related Cdc42-binding kinase acts as a Cdc42 effector in promoting cytoskeletal reorganization. *Mol. Cell. Biol.* **18**, 130–140 (1998).
- Watanabe, N. *et al.* p140mDia, a mammalian homolog of *Drosophila* diaphanous, is a target protein for Rho small GTPase and is a ligand for profilin. *EMBO J.* **16**, 3044–3056 (1997).
- Castrillon, D. & Wasserman, S. Diaphanous is required for cytokinesis in *Drosophila* and shares domains of similarity with the products of the limb deformity gene. *Development* **120**, 3367–3377 (1994).
- Uehata, M. *et al.* Calcium sensitization of smooth muscle mediated by a Rho-associated protein kinase in hypertension. *Nature* **389**, 990–994 (1997).
- Niwa, H., Yamamura, K. & Miyazaki, J. Efficient selection for high-expression transfectants with a novel eukaryotic vector. *Gene* **108**, 193–200 (1991).
- Andreassen, P., Palmer, D., Werner, M. & Margolis, R. Telophase disc: a new mammalian mitotic organelle that bisects telophase cells with a possible function in cytokinesis. *J. Cell Sci.* **99**, 523–534 (1991).

Supplementary information is available on *Nature's* World-Wide Web site (<http://www.nature.com>).

Acknowledgements. We thank S. Yonemura and I. Mabuchi for critically reading the manuscript and H. A. Popiel for editing it; H. Fuyuhiko and K. Nonomura for technical assistance; and T. Arai, H. Nose and K. Okuyama for secretarial assistance. This work was supported in part by a grant from the Ministry of Education, Sciences, Sports and Culture of Japan and by a grant for the Human Frontier Science Program. P.M. was supported in part by the Ciba-Geigy Foundation.

Correspondence and requests for materials should be addressed to S.N. (e-mail: snaru@mfour.med.kyoto-u.ac.jp). The nucleotide sequences encoding citron kinase have been deposited in GenBank under accession numbers AF070065 and AF070066.

EEA1 links PI(3)K function to Rab5 regulation of endosome fusion

Anne Simonsen^{*†}, Roger Lippé^{‡‡#}, Savvas Christoforidis^{‡‡#}, Jean-Michel Gaullier^{*}, Andreas Brech[§], Judy Callaghan^{||}, Ban-Hock Toh^{||}, Carol Murphy^{‡‡#}, Marino Zerial^{‡‡#} & Harald Stenmark^{*}

^{*} Department of Biochemistry, The Norwegian Radium Hospital, Montebello, N-0310 Oslo, Norway

[‡] EMBL, Meyerhofstrasse 1, D-69012 Heidelberg, Germany

[§] EM-unit, Institute of Biology, PO Box 1050, Blindern, N-0316 Oslo, Norway

^{||} Department of Pathology and Immunology, Monash Medical School, Prahran, Victoria 3181, Australia

[#] Max Planck Institute for Molecular Cell Biology and Genetics, Dresden, 01307, Germany

[†] These authors contributed equally to this work

GTPases and lipid kinases regulate membrane traffic along the endocytic pathway by mechanisms that are not completely understood^{1–4}. Fusion between early endosomes requires phosphatidylinositol-3-OH kinase (PI(3)K) activity^{5–7} as well as the small GTPase Rab5 (ref. 8). Excess Rab5–GTP complex restores endosome fusion when PI(3)K is inhibited^{5,9}. Here we identify the early-endosomal autoantigen EEA1 (refs 10–12) which binds the PI(3)K product phosphatidylinositol-3-phosphate, as a new Rab5 effector that is required for endosome fusion. The association of EEA1 with the endosomal membrane requires Rab5–GTP and PI(3)K activity, and excess Rab5–GTP stabilizes the membrane association of EEA1 even when PI(3)K is inhibited. The identification of EEA1 as a direct Rab5 effector provides a molecular link between PI(3)K and Rab5, and its restricted distribution to early endosomes¹⁰ indicates that EEA1 may confer directionality to Rab5-dependent endocytic transport.

EEA1 binds to phosphatidylinositol-3-phosphate (PtdIns(3)-P)^{11,12} and localizes together with Rab5 on endosomes^{10,12,13}. Because a GTP-hydrolysis-deficient mutant of Rab5 can counteract the effect of the PI(3)K inhibitor wortmannin on endosome fusion^{5,9}, we determined whether EEA1 might physically interact with Rab5. Using the yeast two-hybrid system (Table 1), we first found that wild-type Rab5 and a mutant with preferential affinity for GDP, Rab^{S34N}, in which serine 34 is converted to asparagine, showed minimal interaction with EEA1. Remarkably, the GTPase-deficient mutant Rab5^{Q79L} interacted strongly with EEA1, indicating that the GTP-bound form of Rab5 may recognize EEA1. We detected no interaction between EEA1 and the corresponding GTPase-deficient mutants of other Rab proteins (Rab3A^{Q81L}, Rab3C^{Q81L}, Rab4A^{Q67L}, Rab4B^{Q67L}, Rab6^{Q72L}, Rab7^{Q67L} and Rab11^{Q70L}) (Table 1), indicating that EEA1 interacts specifically with Rab5.

A deletion analysis showed that both amino- and carboxy-terminal EEA1 fragments (EEA1-NT and EEA1-CT, respectively; Fig. 1a) can interact with Rab5^{Q79L} in the two-hybrid system (Table 1). We first found that EEA1-NT (Fig. 1a) interacts with

^{*} Present address: University of Ioannina Medical School, 45110 Ioannina, Greece.

Table 1 Interactions between EEA1 and Rab proteins in the two-hybrid system

	EEA1	Rab5 ^{Q79L}	Rab5 ^{S34N}
Rab5	0.53 ± 0.21		
Rab5 ^{Q79L}	101 ± 33.3		
Rab5 ^{S34N}	0.15 ± 0.05		
Rab3C ^{Q81L}	0.07 ± 0.01		
Rab3C ^{Q81L}	0.26 ± 0.13		
Rab4A ^{Q67L}	0.12 ± 0.01		
Rab4B ^{Q67L}	0.05 ± 0.04		
Rab6 ^{Q72L}	0.04 ± 0.01		
Rab7 ^{Q67L}	0.06 ± 0.02		
Rab11 ^{Q70L}	0.07 ± 0.01		
		Rab5 ^{Q79L}	Rab5 ^{S34N}
EEA1 _{1,257-1,411*}	25.6 ± 0.9	0.11 ± 0.07	
EEA1 _{1,277-1,411*}	32.0 ± 11.2	0.09 ± 0.04	
EEA1 _{1,325-1,411*}	0.77 ± 0.02	0.11 ± 0.06	
EEA1 _{1,277-1,357*}	15.4 ± 1.5	0.21 ± 0.15	
EEA1 _{1,277-1,348*}	4.16 ± 0.51	0.21 ± 0.06	
EEA1 _{1,307-1,357*}	0.13 ± 0.02	0.14 ± 0.03	
EEA1 ₁₋₂₀₉	512 ± 43.1	0.17 ± 0.02	
EEA1 ₁₋₂₀₉ ^{C46S}	0.08 ± 0.01	—	
EEA1 ₁₋₁₅₃	95.2 ± 13.6	0.08 ± 0.01	
EEA1 ₁₋₉₁	17.4 ± 0.97	0.07 ± 0.01	

Results were obtained from yeast two-hybrid assays by measurement of *lacZ* reporter activity. L40 reporter yeast cells were transformed with Rab constructs in plasmid pLexA, and EEA1 constructs in plasmid pGAD, or vice versa where indicated with an asterisk. The cells were grown to *A*₆₀₀ values of roughly 1.0 in synthetic medium lacking tryptophan and leucine. β-Galactosidase activity was then measured using *o*-nitrophenyl-β-D-galactopyranoside as a substrate. β-Galactosidase activities (in relative units) are presented as mean values ± deviations between duplicate transformants.

Rab5^{Q79L} and not with Rab5^{S34N}. This interaction presumably involves the C₂H₂ zinc-finger motif of EEA1, as a point mutation in this motif (producing EEA1-NT^{C46S}) abolished the interaction with Rab5^{Q79L}, and a small fragment containing the zinc finger (EEA1₁₋₉₁) retained the ability to interact. We further found that, like EEA1-NT, EEA1-CT, which contains a PtdIns(3)P-binding FYVE finger¹², interacts with Rab5^{Q79L} but not with Rab5^{S34N}. The entire FYVE finger could be removed with only a weak reduction in Rab5^{Q79L} binding (Table 1). The minimal Rab5-binding region of EEA1-CT resides within residues 1,277–1,348, which constitute the domain immediately N-terminal of the FYVE finger. The region encompassing amino-acid residues 1,306–1,340 of EEA1 is 29% identical and 43% similar to the Rab5-binding region¹⁴ of the Rab5 effector Rabaptin-5 (results not shown), indicating that the Rab5-binding regions of EEA1-CT and Rabaptin-5 may be structurally related.

We next confirmed the Rab5–EEA1 interactions biochemically. EEA1 from bovine brain cytosol bound specifically to immobilized Rab5 fused to maltose-binding protein (MBP–Rab5). We detected binding only in the presence of the non-hydrolysable GTP analogue GTP-γS, and not in the presence of GDP or the absence of nucleotide (Fig. 1b). In agreement with the two-hybrid data, we detected only background-level interaction of EEA1 with MBP–Rab4 and with MBP–Rab6, even in the presence of GTP-γS. Moreover, recombinant His₆–EEA1 protein bound to an immobilized glutathione S-transferase (GST)–Rab5 fusion protein in the GTPγS-bound form, but not in the GDP-bound form (Fig. 1c), showing that the interaction is direct and independent of other cytosolic factors. Finally, we also demonstrated GTPγS-specific interactions between GST–Rab5 and MBP–EEA1-NT (Fig. 1d) or MBP–EEA1-CT (Fig. 1e), confirming the results from the two-hybrid assays.

Next we determined whether EEA1 functions in early-endosome fusion. Expression of Rab5^{Q79L} leads to the expansion of early endosomes in BHK cells because of increased fusion activity (Fig. 2a)¹⁵. Although the expression of Myc-epitope-tagged EEA1-NT with Rab5^{Q79L} had no effect (results not shown), the coexpression of Myc-tagged EEA1-CT (Fig. 2b) counteracted the activity of the Rab5 mutant, resulting in the clustering of small endocytic structures (Fig. 2b, inset) often located in the periphery of the cell. In contrast, the FYVE-finger mutant EEA1-CT^{C1358S}, which does not

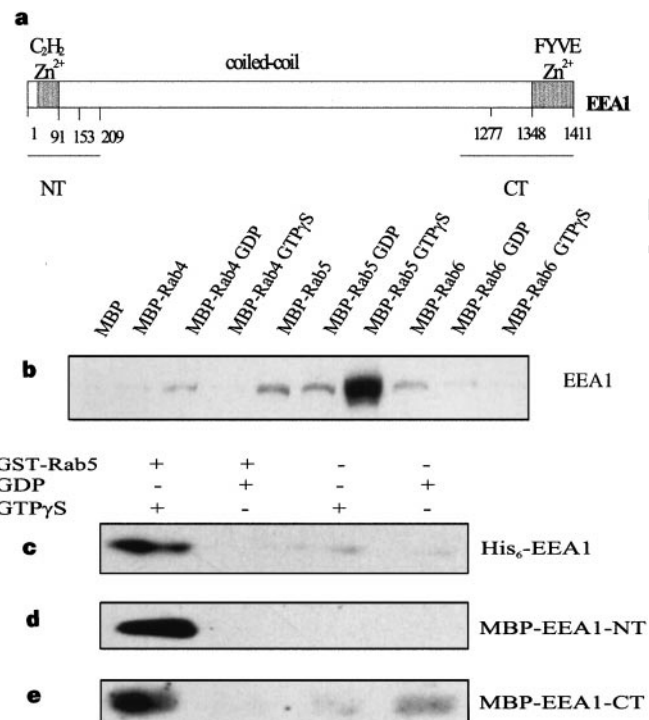


Figure 1 Biochemical interaction between EEA1 and Rab5. **a**, Representation of wild-type EEA1, with the C₂H₂ and FYVE zinc fingers indicated. The EEA1 constructs are indicated by their amino-acid numbers. The point mutants used were C46S in the C₂H₂ finger and C1,358S in the FYVE finger. We use the terms EEA1-NT for EEA1₁₋₂₀₉ and EEA1-CT for EEA1_{1,277-1,411}. **b**, MBP–Rab4, MBP–Rab5 or MBP–Rab6, immobilized on Affi-Gel, were either nucleotide-free or loaded with GDP or GTP-γS and then incubated with bovine brain cytosol to study their binding to EEA1. **c–e**, Glutathione-agarose beads, with or without bound GST–Rab5, were incubated with GDP or GTP-γS and then mixed with recombinant His₆–EEA1 (**c**), MBP–EEA1-NT (**d**), or MBP–EEA1-CT (**e**). Bound proteins were eluted with reduced glutathione. Bound proteins in **b** and eluted fractions in **c–e** were analysed by SDS-PAGE and immunoblotting with anti-EEA1 antiserum (**b–d**) or anti-MBP antibodies (**e**).

bind to endosomes¹³, did not affect the expansion of early endosomes (Fig. 2c), indicating that the effect of EEA1-CT requires its binding to endosomes. We studied the effect of EEA1-CT on early endosomes under normal conditions (that is, in the absence of the stimulatory Rab5 mutant) by electron microscopy. Cells expressing EEA1-CT contained many small, early-endocytic profiles (Fig. 2d), which were significantly smaller than the early endosomes of untransfected cells (Fig. 2e). These results indicate that the expression of EEA1-CT affects the size of normal as well as Rab5^{Q79L}-containing early endosomes.

To determine whether EEA1-CT inhibits early-endosome fusion directly, we used an *in vitro* endosome fusion assay based on the detection of complexes formed between ligands internalized into two separate early endosome populations^{8,16}. We prepared cytosol from baby hamster kidney (BHK) cells overexpressing EEA1-CT or EEA1-CT^{C1358S} and tested this cytosol in the fusion assay in the presence of cytosol from HeLa cells. The fusion activity was cytosol-dependent (Fig. 3a). We detected 60% inhibition of fusion when early endosomes were incubated in the presence of cytosol containing EEA1-CT, but not in the presence of cytosol containing EEA1-CT^{C1358S}. An anti-EEA1 serum, but not its corresponding preimmune serum, inhibited early-endosome fusion by ~80% when added directly to the fusion reaction (Fig. 3b). Addition of the peptide against which the antiserum had been raised completely rescued this inhibition, indicating that the blocking effect of the antibodies was specific. Depletion of EEA1 from cytosol caused a

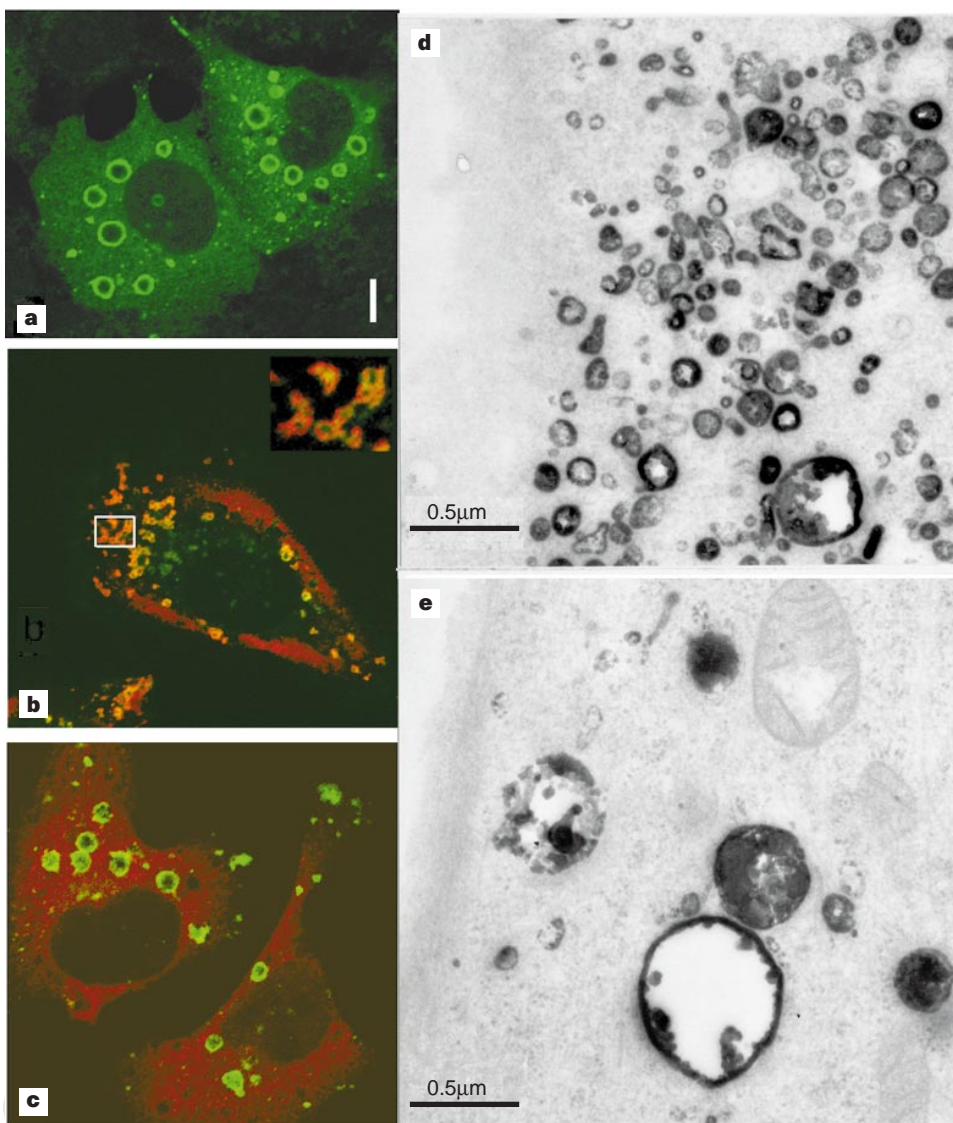


Figure 2 The C-terminal part of EEA1 inhibits basal and Rab5-stimulated early-endosome fusion *in vivo*. **a–c**, Confocal immunofluorescence micrographs showing the intracellular localization of Rab5^{Q79L} (green) and Myc-EEA1-CT (red) in BHK cells transfected with Rab5^{Q79L} (**a**), Rab5^{Q79L} + Myc-EEA1-CT (**b**), or Rab5^{Q79L} + Myc-EEA1-CT^{C1,358S} (**c**). Yellow indicates colocalization. Scale bar in **a**, 5 μm. **d, e**, Electron micrographs of BHK cells after internalization of horseradish peroxidase for 10 min at 37 °C. Myc-EEA1-CT-expressing cells show many small endocytic profiles (**d**), in contrast to early endosomes in control cells (**e**).

somewhat lower inhibition of fusion (50–70%), and this effect could be rescued on addition either of an EEA1-enriched fraction purified from cytosol or of recombinant EEA1 (Fig. 3b). These data indicate that EEA1 is required for homotypic early-endosome fusion.

The observation that EEA1 functions in endosome fusion is intriguing in view of previous findings that PI(3)K activity is required both for endosome fusion^{5–7,17} and for EEA1 binding to endosomes^{11,12}. We found that *in vitro* endosome fusion was inhibited ~70% by 100 nM wortmannin, a PI(3)K inhibitor. This inhibition was counteracted by Rab5 (incorporated as an XTP-binding mutant, Rab5^{D136N}, loaded with XTP-γS or XTP¹⁸), which stimulated fusion strongly (Fig. 3b). The effect of Rab5 (–XTPγS) is probably the result of mass action of activated Rab5 rather than an effect of neutralization of the inhibition by wortmannin⁹. The finding that EEA1 depletion from cytosol only partially inhibited fusion (Fig. 3b) could be explained by the presence of residual EEA1 on the endosome membrane, in agreement with previous localization studies¹⁰. Fusion after EEA1 depletion and wortmannin treatment was less than after either treatment alone, indicating that the two treatments had an additive effect (Fig. 3b). The presence of

Rab5^{Q79L} + Myc-EEA1-CT^{C1,358S} (**c**). Yellow indicates colocalization. Scale bar in **a**, 5 μm. **d, e**, Electron micrographs of BHK cells after internalization of horseradish peroxidase for 10 min at 37 °C. Myc-EEA1-CT-expressing cells show many small endocytic profiles (**d**), in contrast to early endosomes in control cells (**e**).

Rab5-XTP restored fusion up to only 35% of the basal level under these conditions. Rab5-XTPγS had a similar effect to Rab5-XTP (results not shown). The effect of Rab5-XTP and Rab5-XTPγS is probably due to their action on residual EEA1 present in the fusion reaction. These results show that EEA1 is essential for Rab5-dependent endosome fusion, and that its activity is regulated by PI(3)K.

Given that EEA1 can bind to PtdIns(3)P¹² as well as to activated Rab5, we determined whether Rab5-GTP can counteract the inhibition of early-endosome fusion induced by wortmannin by stabilizing EEA1 on the membrane. For this purpose we used Madin–Darby canine kidney (MDCK) cells expressing Rab5^{Q79L} (Fig. 4)¹⁹. Although EEA1 was abundant in the cytosol (Fig. 4, lane 1) as well as in the membrane fraction (lane 2) of untransfected cells, most EEA1 was membrane-bound in Rab5^{Q79L}-expressing cells (lanes 5, 6). Most important, on treatment with wortmannin, EEA1 efficiently dissociated from the membranes of untransfected cells (lanes 3, 4)^{11,12}, whereas a significant fraction remained membrane-bound in the Rab5^{Q79L}-expressing cells (lanes 7, 8). These data indicate that EEA1 binding to endosomes is dependent on PtdIns(3)P as well as on Rab5-GTP and that the presence of

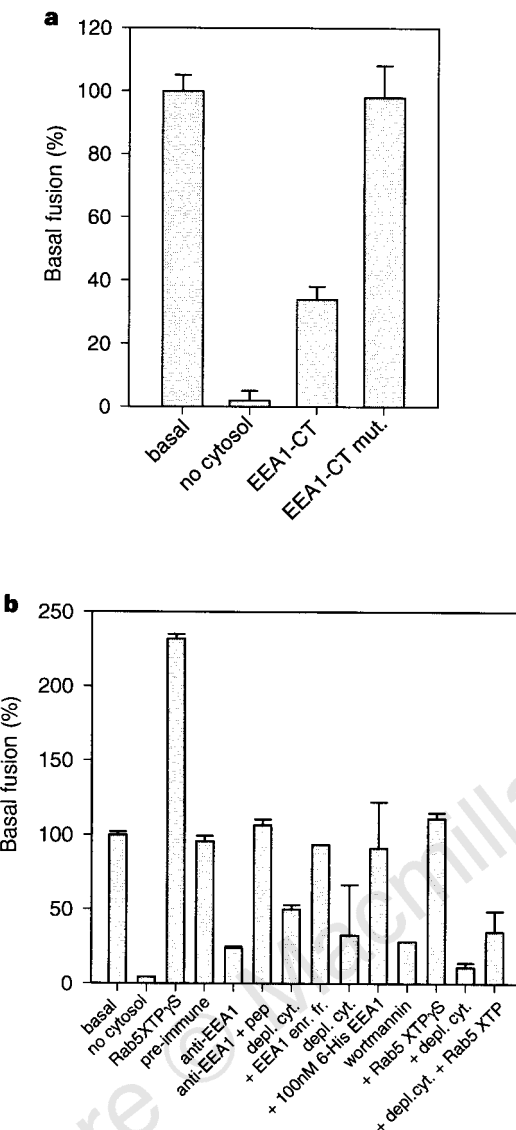


Figure 3 EEA1 is required for early endosome fusion *in vitro*. Homotypic early endosome fusion in the presence of (a) cytosol from BHK cells transfected with EEA1-CT or EEA1-CT^{C136S} or (b) preimmune serum, anti-EEA1 serum, anti-EEA1 serum + EEA1 N-terminal peptide added, EEA1-depleted HeLa cell cytosol in the absence or presence of recombinant His₆-EEA1, EEA1-enriched cytosolic fraction, or HeLa cell cytosol incubated with wortmannin in the absence or presence of Rab5^{D136N}-XTP γ S or Rab5^{D136N}-XTP (75 nM). Note that the four right-most columns of panel b all represent fusion experiments done in the presence of wortmannin. All fusion activities were calculated as a percentage of that occurring in the presence of cytosol and an ATP-regeneration system (basal fusion). This fusion was typically 5–10% of maximal fusion, defined as the signal detected in the presence of Triton X-100. Fusion in the absence of ATP was less than 10% of basal fusion (data not shown). Error bars represent deviations between duplicates. Note the different scale in a and b.

activated Rab5 on the membrane can compensate for the lack of PtdIns(3)P in the presence of wortmannin.

The findings that EEA1 binds to activated Rab5 and regulates Rab5-dependent membrane fusion establish EEA1 as a new Rab5 effector. The two Rab5 effectors, EEA1 and Rabaptin-5 (ref. 20), are likely to have distinct functions; they are structurally different, and EEA1 is much more abundant than Rabaptin-5 on early endosomes^{10,20}. Because Rab5 is found not only on early endosomes but also at the plasma membrane and on clathrin-coated vesicles^{21,22}, other molecules are needed to confer directionality to Rab5-dependent membrane fusion. The restricted localization

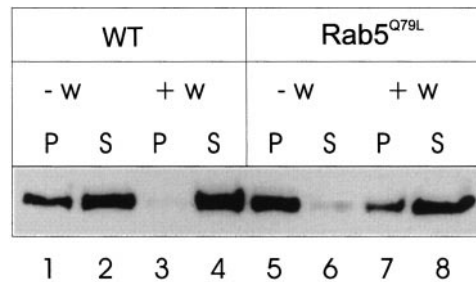


Figure 4 The membrane association of EEA1 is regulated by Rab5 and PI(3)K. Wild-type (lanes 1–4) or Rab5^{Q79L}-transfected¹⁹ (lanes 5–8) MDCK I cells in 9-cm plastic dishes were incubated for 30 min at 37 °C in the absence (lanes 1, 2, 5, 6) or presence (lanes 3, 4, 7, 8) of 100 nM wortmannin. The cells were then homogenized, and postnuclear supernatants were centrifuged at 100,000g for 30 min (ref. 20). The pellet (lanes 1, 3, 5 and 7) and supernatant fractions (lanes 2, 4, 6 and 8) were analysed by SDS-PAGE followed by immunoblotting with anti-EEA1 antibodies.

of EEA1 to early endosomes indicates that it may fulfil such a role.

The following model may explain our results. EEA1 may be recruited initially to early endosomes through binding to Rab5-GTP, and may then be stabilized further on the membrane by interaction of its FYVE finger with PtdIns(3)P. As the affinity of EEA1 for either of these components may be low, or because the components are labile, the binding of EEA1 to membranes would be inefficient in the absence of either Rab5-GTP or PtdIns(3)P. Our model predicts that the presence of either Rab5-GTP or PtdIns(3)P would be sufficient to recruit EEA1 to membranes if present in excessive amounts. This can be seen in the presence of excess Rab5-GTP (Fig. 4) and in experiments using liposomes (with excess PtdIns(3)P)^{11,12}. Our results indicate that one important function of PI(3)K in the endocytic pathway may be to ensure the efficient attachment of the new Rab5 effector EEA1 to membranes. EEA1 is therefore the first molecular link between PI(3)K and Rab5 in endocytic membrane traffic. □

Methods

Antibodies and recombinant proteins. Anti-EEA1 was obtained by immunizing a rabbit with a peptide corresponding to the 16 N-terminal residues of EEA1 coupled to diphtheria toxin. The antiserum was affinity-purified on recombinant MBP-EEA1-NT immobilized on Affi-Gel (Bio-Rad). For expression of GST-Rab5, Rab5 complementary DNA was cloned into pGEX-5x-3 (Pharmacia). In order to express His₆-EEA1 in insect cells, we cloned Myc-EEA1¹³ into pFAST-Bac-HTa (Gibco-BRL) and constructed a recombinant baculovirus according to the manufacturer's instructions. For expression of MBP-EEA1-NT and MBP-EEA1-CT, we cloned the respective EEA1 constructs into pMAL-C2 (New England Biolabs). The *Escherichia coli* expression plasmids were transformed into *E. coli* BL-21(DE3) cells. Expression and protein purification were according to the manufacturers' instructions.

Measurement of protein-protein interactions with the yeast two-hybrid system. Yeast two-hybrid constructs were prepared in the 'bait' vector pLexA/pBTM116 (ref. 23) and the 'prey' vector pGAD-GH (Clontech) using Rab5 (ref. 21) and EEA1 (ref. 10) sequences with the indicated mutations. L40 yeast reporter cells²³ were transformed as indicated in Table 1, and liquid β-galactosidase assays²⁰ were done on duplicate transformants.

Rab5 affinity chromatography. For binding of cytosolic EEA1, MBP-Rab5 was coupled to Affi-Gel 15 (Bio-Rad) and then loaded with GDP or GTP-γS¹⁶. The beads were further incubated with a 0–40% (NH₄)₂SO₄-precipitated fraction of bovine brain cytosol for 1.5 h at 4 °C, and bound proteins were analysed by SDS-PAGE and immunoblotting with anti-EEA1 antibodies. To detect binding of recombinant EEA1, glutathione-agarose beads (Pharmacia) were incubated in the absence or presence of GST-Rab5 (2 μM) for 1 h at 37 °C in a buffer containing 10 μM GDP or GTP-γS. Recombinant His₆-EEA1 (600 nM), MBP-EEA1-NT (1 μM) or MBP-EEA1-CT (43 nM) was added to the beads for 1 h at 4 °C in the presence of 10 mg ml⁻¹ albumin. Bound

proteins were subsequently eluted with 10 mM reduced glutathione for 20 min at room temperature and analysed by SDS-PAGE and immunoblotting with anti-EEA1 or anti-MBP antibodies.

Transient expression in BHK cells. EEA1 and Rab5 constructs were cloned behind the T7 promoter of plasmid pGEM-1 (Promega) and expressed in BHK-21 cells using the T7 RNA polymerase recombinant vaccinia virus system and lipofection as described²⁴. Cells were analysed 4 h after transfection.

Confocal immunofluorescence microscopy. BHK cells grown on coverslips were transiently transfected, fixed and stained for immunofluorescence microscopy as described²⁰. Myc-tagged proteins were detected using the 9E10 mouse monoclonal antibody²⁵, and Rab5^{Q79L} was visualized with affinity-purified anti-Rab5 antibodies²¹, followed by rhodamine- or fluorescein-conjugated secondary antibodies against mouse or rabbit IgG (Jackson ImmunoResearch). Coverslips were examined using a Zeiss confocal scanning laserbeam microscope.

Electron microscopy. BHK cells in 3-cm plastic dishes were incubated for 10 min at 37 °C with horseradish peroxidase (5 mg ml⁻¹, type VI, Sigma), then washed extensively with ice-cold phosphate-buffered saline and fixed with 2% glutaraldehyde in 0.1% sodium cacodylate, pH 7.2. The cells were then processed for electron microscopy²⁶ and 120–250-nm sections were examined in a JEOL 1200 electron microscope.

Assay of early-endosome fusion. Two early-endosome-enriched fractions containing, respectively, biotinylated transferrin or anti-transferrin were separately prepared from HeLa cells, and the fusion was assayed in the presence of HeLa cell cytosol containing an ATP-regenerating system, unless otherwise specified, as described¹⁶. For immunodepletion of EEA1, we used protein-A-Sepharose preincubated with anti-EEA1 antibodies, as described for immunodepletion of Rabaptin-5 (ref. 16). Immunoblotting experiments indicated that >90% of cytosolic EEA1 was depleted under these conditions. The EEA1-enriched fraction used in rescue experiments was obtained by mono-Q ion-exchange chromatography of a 30–40% ammonium sulphate fraction from bovine brain cytosol¹⁶.

Received 1 June; accepted 13 July 1998.

- Novick, P. & Zerial, M. The diversity of Rab proteins in vesicle transport. *Curr. Opin. Cell Biol.* **9**, 496–504 (1997).
- Olkkinen, V. M. & Stenmark, H. Role of rab GTPases in membrane traffic. *Int. Rev. Cytol.* **176**, 1–85 (1997).
- Roth, M. G. & Sternweis, P. C. The role of lipid signaling in constitutive membrane traffic. *Curr. Opin. Cell Biol.* **9**, 519–526 (1997).
- De Camilli, P., Emr, S. D., McPherson, P. S. & Novick, P. Phosphoinositides as regulators in membrane traffic. *Science* **271**, 1533–1539 (1996).
- Li, G. *et al.* Evidence for phosphatidylinositol 3-kinase as a regulator of endocytosis via activation of Rab5. *Proc. Natl Acad. Sci. USA* **92**, 10207–10211 (1995).
- Jones, A. T. & Clague, M. J. Phosphatidylinositol 3-kinase activity is required for early endosome fusion. *Biochem. J.* **311**, 31–34 (1995).
- Spiro, D. J., Boll, W., Kirchhausen, T. & Wessling-Resnick, M. Wortmannin alters the transferrin receptor endocytic pathway *in vivo* and *in vitro*. *Mol. Biol. Cell* **7**, 355–367 (1996).
- Gorvel, J. P., Chavrier, P., Zerial, M. & Gruenberg, J. rab5 controls early endosome fusion *in vitro*. *Cell* **64**, 915–925 (1991).
- Jones, A. T., Mills, I. G., Scheidig, A. J., Alexandrov, K. & Clague, M. J. Inhibition of endosome fusion by wortmannin persists in the presence of activated rab5. *Mol. Biol. Cell* **9**, 323–332 (1998).
- Mu, F. T. *et al.* EEA1, an early endosome-associated protein. EEA1 is a conserved alpha-helical peripheral membrane protein flanked by cysteine “fingers” and contains a calmodulin-binding IQ motif. *J. Biol. Chem.* **270**, 13503–13511 (1995).
- Patki, V., Virbasius, J., Lane, W. S., Toh, B. H., Shpetner, H. S. & Corvera, S. Identification of an early endosomal protein regulated by phosphatidylinositol 3-kinase. *Proc. Natl Acad. Sci. USA* **94**, 7326–7330 (1997).
- Gaulier, J.-M. *et al.* A functional PtdIns(3)P-binding motif. *Nature* **394**, 433–434 (1998).
- Stenmark, H., Aasland, R., Toh, B. H. & D’Arrigo, A. Endosomal localization of the autoantigen EEA1 is mediated by a zinc-binding FYVE finger. *J. Biol. Chem.* **271**, 24048–24054 (1996).
- Vitale, G. *et al.* Distinct Rab-binding domains mediate the interaction of rabaptin-5 with GTP-bound rab4 and rab5. *EMBO J.* **17**, 1941–1951 (1998).
- Stenmark, H., Parton, R. G., Steele-Mortimer, O., Lütcke, A., Gruenberg, J. & Zerial, M. Inhibition of rab5 GTPase activity stimulates membrane fusion in endocytosis. *EMBO J.* **13**, 1287–1296 (1994).
- Horiuchi, H. *et al.* A novel Rab5 GDP/GTP exchange factor complexed to rabaptin-5 links nucleotide exchange to effector recruitment and function. *Cell* **90**, 1149–1159 (1997).
- Shpetner, H., Joly, M., Hartley, D. & Corvera, S. Potential sites of PI-3 kinase function in the endocytic pathway revealed by the PI-3 kinase inhibitor, wortmannin. *J. Cell Biol.* **132**, 595–605 (1996).
- Rybini, V. *et al.* GTPase activity of Rab5 acts as a timer for endocytic membrane fusion. *Nature* **383**, 266–269 (1996).
- D’Arrigo, A., Bucci, C., Toh, B. H. & Stenmark, H. Microtubules are involved in bafilomycin A1-induced tubulation and Rab5-dependent vacuolation of early endosomes. *Eur. J. Cell Biol.* **72**, 95–103 (1997).
- Stenmark, H., Vitale, G., Ullrich, O. & Zerial, M. Rabaptin-5 is a direct effector of the small GTPase Rab5 in endocytic membrane fusion. *Cell* **83**, 423–432 (1995).
- Chavrier, P., Parton, R. G., Hauri, H. P., Simons, K. & Zerial, M. Localization of low molecular weight GTP binding proteins to exocytic and endocytic compartments. *Cell* **62**, 317–329 (1990).
- Bucci, C. *et al.* The small GTPase rab5 functions as a regulatory factor in the early endocytic pathway. *Cell* **70**, 715–728 (1992).
- Vojtek, A. B., Hollenberg, S. M. & Cooper, J. A. Mammalian Ras interacts directly with the serine/threonine kinase Raf. *Cell* **74**, 205–214 (1993).

- Stenmark, H., Bucci, C. & Zerial, M. Expression of Rab GTPases using recombinant vaccinia viruses. *Methods Enzymol.* **257**, 155–164 (1995).
- Evan, G. I., Lewis, G. K., Ramsay, G. & Bishop, J. M. Isolation of monoclonal antibodies specific for human c-myc proto-oncogene product. *Mol. Cell. Biol.* **5**, 3610–3616 (1985).
- Toote, J. & Hollinshead, M. Tubular early endosome networks in AtT20 and other cells. *J. Cell Biol.* **115**, 635–653 (1991).

Acknowledgements. We thank E. Rønning for technical assistance; D. Warren for help with the baculovirus system; N. Salmon and T. Nordeng for help with confocal microscopy; V. Rybin for providing the Rab5D^{365N}-Rep1 complex; E. Kolpakova for anti-MBP antibodies; and H. McBride, S. Olsnes, K. Sandvig and B. Sønnichsen for comments on the manuscript. H.S. was supported by the Top Research Programme, the Research Council of Norway, the Norwegian Cancer Society and the Novo Nordisk Foundation. This work was supported by a European Community TMR grant (to H.S. and M.Z.).

Correspondence and requests for materials should be addressed to H.S. (e-mail: stenmark@ulrik.uio.no).

Transcriptional activators direct histone acetyltransferase complexes to nucleosomes

Rhea T. Utley*, Keiko Ikeda**†, Patrick A. Grant*, Jacques Côté‡, David J. Steger*, Anton Eberharter*, Sam John* & Jerry L. Workman*

* Howard Hughes Medical Institute, Department of Biochemistry and Molecular Biology and The Center for Gene Regulation, 306 Althouse Laboratory, Pennsylvania State University, University Park, Pennsylvania 16802-4500, USA

† Department of Biology, Jichi Medical School, Minamikawachi, Kawachi, Tochigi 329-04, Japan

‡ Laval University Cancer Research Center, Hôtel-Dieu de Québec, Québec G1R-2J6, Canada

Transcriptional co-activators were originally identified as proteins that act as intermediaries between upstream activators and the basal transcription machinery. The discovery that co-activators such as *Tetrahymena* and yeast Gcn5^{1,2}, as well as human p300/CBP^{3,4}, pCAF⁵, Src-1⁶, ACTR⁷ and TAFII250⁸, can acetylate histones suggests that activators may be involved in targeting acetylation activity to promoters. Several histone deacetylases have been linked to transcriptional co-repressor proteins⁹, suggesting that the action of both acetylases and deacetylases is important in the regulation of many genes. Here we demonstrate the binding of two native yeast histone acetyltransferase (HAT) complexes to the herpesvirus VP16 activation domain and the yeast transcriptional activator Gcn4, and show that it is their interaction with the VP16 activation domain that targets Gal4–VP16-bound nucleosomes for acetylation. We find that Gal4–VP16-driven transcription from chromatin templates is stimulated by both HAT complexes in an acetyl CoA-dependent reaction. Our results demonstrate the targeting of native HAT complexes by a transcription-activation domain to nucleosomes in order to activate transcription.

We previously identified four multisubunit native yeast HAT complexes². Two of these complexes, SAGA and Ada, preferentially acetylate nucleosomal histone H3 and contain Gcn5 as the catalytic histone acetyltransferase subunit. SAGA (for Spt-Ada-Gcn5-acetyltransferase) is an 1,800K HAT complex which also contains Ada2, Ada3, Ada5/Spt20, Spt3 and Spt7 (ref. 2) explaining the functional link between the Ada and Spt classes of transcription regulator^{10,11}. The 800K Ada complex contains Ada2 and Ada3 as well as Gcn5, but none of the Spt proteins². Two HATs, formerly termed complex 2, which acetylates histones H4 and H2A, and complex 3, with a substrate preference for histone H3 (ref. 2), were purified and named NuA4 (for nucleosomal acetyltransferase of histone H4) and NuA3, respectively.

Acetylation of histone H3 is stimulated specifically in the promoter regions of Gcn5-dependent genes¹², indicating that promo-